ON THE OLIGOMERIC STATE OF DJ-1 PROTEIN AND ITS MUTANTS ASSOCIATED WITH PARKINSON'S DISEASE: A COMBINED COMPUTATIONAL AND *IN VITRO* STUDY

Fernando E. Herrera[1]*, Silvia Zucchelli[2,3]*, Aneta Jezierska[1,4]*, Zeno Scotto Lavina[2,3], Stefano Gustincich[2,3] and Paolo Carloni[1]

*contributed equally

International School for Advanced Studies (SISSA), INFM DEMOCRITOS, Via Beirut 2-4, 34014 Trieste, Italy [1], Sector of Neurobiology[2], The Giovanni Armenise-Harvard Foundation Laboratory[3], AREA Science Park, S.S. 14, Km 163, 5, Basovizza, 34012 Trieste, Italy (on leave from: University of Wrocław, Faculty of Chemistry, 14 F. Joliot-Curie, 50-383 Wrocław, Poland) [4]

Running head: DJ-1 protein and its mutants associated with PD

Address correspondence to: Paolo Carloni, International School for Advanced Studies, Via Beirut 2-4, 34014 Trieste, Italy. Tel: +39-040-3787407, Fax: +39-040-3787528; E-mail: carloni@sissa.it and Stefano Gustincich, International School for Advanced Studies AREA Science Park, S.S. 14, Km 163.5, Basovizza, 34012 Trieste, Italy. Tel: +39-040-3756505, Fax: +39-040-3756502; E-mail: gustinci@sissa.it.

Mutations in the DJ-1 protein are present in patients suffering from familiar Parkinson's disease (PD) (1, 2).

Here we use computational methods and biological assays to investigate the relationship between DJ-1 missense mutations and the protein oligomeric state. Molecular dynamics (MD) calculations suggest that: (i) the structure of DJ-1 wild-type (WT) in aqueous solution, in both oxidized and reduced forms, is similar to the crystal structure of the reduced form (3, 4); (ii) the PD-causing M26I variant is structurally similar to the WT, consistent with the experimental evidence showing the protein is a dimer as WT ((5-7) and in this work); (iii) R98Q is structurally similar to the WT, consistent with the fact that this is a physiological variant (8); (iv) the L166P monomer rapidly evolves towards a conformation significantly different than WT, suggesting a change in its ability to oligomerize (3, 4).

Our combined computational and experimental approach is next used to identify a mutant (R28A) that, in contrast to L166P, destabilizes the dimer subunit-subunit interface without significantly changing secondary structure elements.

Parkinson's Disease (PD)[#] is the second most common progressive neurodegenerative disorder, affecting 1-2% of all individuals above the age of 65 (9-12). PD is characterized by muscle rigidity, resting tremor, bradykinesia and gait disturbance with dysequilibrium. The neuropathological hallmark in *post mortem* brains is the selective degeneration of specific subsets of mesencephalic dopaminergic cells and the formation of cytoplasmic aggregates called Lewy bodies.

The identification of genes associated with rare forms of early-onset familial PD has provided crucial insights into the mechanism of the pathogenesis. Several loci have been mapped for monogenic forms of PD and genes have been identified (1). By studying two families from genetically isolated communities, two mutations in the PARK7/DJ-1 gene were found to be associated with autosomal recessive early-onset PD (13).

DJ-1 encodes for a highly conserved, ubiquitously expressed, 189 aminoacid long protein (4) that is involved in multiple cellular processes including sperm maturation, fertilization in rodents and oncogenesis in humans. It is present in the nucleus, cytoplasm, mitochondria and extracellular space of mammalian cells (14-17). Among several potential biochemical activities, DJ-1 has been proven to be a regulator of transcription with the promoter of tyrosine hydroxilase being one of its targets. Furthermore, DJ-1 may act as a redox-regulated chaperone (18). *In vitro* studies showed that the ectopic expression of DJ-1 protects cells from cell death induced by various toxic stimuli including oxidative stress (19, 20). DJ-1 is indeed an indicator of oxidative stress state *in vivo* since it is converted into pI variants in response to small amounts of reactive oxygen species. Interestingly,

1

some pI isoforms are accumulated in PD *post mortem* brains (21, 22).

Several familiar cases prove that DJ-1 loss in humans causes PD: (i) a frame shift and a splice mutation were found in a young-onset PD patient (23); (ii) a Dutch family showed a large homozygous genomic deletion that removed 4 Kb of promoter sequences and the first five exons of the gene (6); (iii) additional PD cases have been described with truncating, splice-site mutations and deletions.

To study the effects of the lack of a functional gene, DJ-1 KO mice and flies were generated. Although they did not show death of dopaminergic neurons, increased vulnerabilities to neurotoxic agents were observed (24-27). Furthermore, embryonic stem cells deficient in DJ-1 and dopaminergic neurons derived *in vitro* from them displayed increased sensitivity to oxidative stress and/or proteasomal inhibition (28).

Interestingly, some PD families present missense mutations of DJ-1 in homozygous and/or heterozygous forms (M26I, E64D, A104T, D149A and L166P) (1, 6, 13, 23, 29, 30). How these mutants change or abolish DJ-1 function is still a matter of debate.

X-ray crystallography (Fig. 1A) showed that WT DJ-1 in the reduced state (that is, in a state in which Cys and/or Met residues are not oxidized (3)) is a homodimer. Each monomer takes a flavodoxin-like Rossman fold (3), containing seven parallel β-strands flanked by nine α-helices. The subunit-subunit interface is stabilized by a large number of hydrophobic interactions, H-bonds and salt bridges (Tab. 1SI). The dimeric state of the protein has been confirmed by both *in vivo* and *in vitro* investigations. It is believed that DJ-1 carries out its function exclusively in the dimeric state (31-34), since the formation of High Molecular Weight (HMW) oligomers and/or inefficient formation of dimeric structures may affect the stability of the protein and/or its affinity for molecular partners in the cell (2, 4, 5).

L166P and M26I are the most studied DJ-1 missense mutations (5, 7, 13, 34, 35).
L166P is very unstable and its expression level, both in transfection studies and in patient lymphoblasts, is lower than WT. This suggests that L166P mutation may induce a loss of DJ-1 function (35-38). The mutant does not form a dimeric structure; instead, it may assemble in HMW oligomers (5, 33, 35). At the structural level, L166 is located in the middle of one of the helical regions of the protein (α8 helix in Fig. 1A and Fig. 2A), thus its mutation to Pro breaks the helix (4, 13, 29, 35). Because the α8 helix forms hydrophobic interactions with a series of residues located at the subunit-subunit interface (V181, K182, L187 of α9 helix and the C-term), such a mutation could affect the stability of the homodimer (4, 29, 36). However, this hypothesis has not yet been proven by *in silico* and/or *in vitro* analysis of the conformational changes in the mutant.

M26I does form dimers but it is a matter of debate whether dimer formation occurs at the same rate as WT or less efficiently. Furthermore, the relevance of these differences, if any, for neurodegeneration is unclear (5, 7, 34). This mutation is located on α1 helix at the subunit-subunit interface (Fig. 1A), therefore it may affect subunit-subunit interactions. However, methionine is structurally and chemically very similar to isoleucine: they are similar in shape and volume and they are both non-polar residues. Thus, the interactions between M26I subunits may well be similar to those of the WT, although structural information for this mutant is lacking.

Here we address these issues by computational approaches along with *in vitro* assays.

Molecular dynamics (MD) simulations based on the DJ-1 WT X-ray structure are carried out on homodimeric and monomeric forms of the WT. An extensive MD study of DJ-1 in the oxidized state has been performed (Fig. 1B) as well as an analysis of the PD-causing mutations L166P and M26I.
Comparison is also made with MD simulations of a physiological variant (R98Q), which is expected to alter neither the DJ-1 fold nor the oligomeric state (8).

Our calculations show that: (i) the reduced and oxidized WT dimers in aqueous solution are very similar to the reduced dimer in the solid state; (ii) M26I in the monomeric and dimeric states

2

maintains completely the fold of the WT; (iii) R98Q is also similar to the WT, fully consistent with the fact that this is a physiological variant; (iv) L166P causes local distortions at α8 helix (Fig. 2A) and at the surface-forming contacts in the dimeric structure. We conclude that this mutation might affect the stability of the dimer by altering the structure of its local environment. Unfortunately, at present, the stability differences (i.e. the free energy differences) between the WT and these mutants cannot be firmly established by calculations alone. However, our conclusions based on the calculations are corroborated by previous biological assays *in vitro* on the WT and its mutants (7, 29, 35). Furthermore, experiments carried out in this work confirm that L166P tends to form multimeric aggregates more than WT does (5, 33, 35).

Finally, our combined computational and experimental methodology is used to engineer a new mutation that, in contrast to L166P, does destabilize the subunit-subunit interactions without affecting the secondary structure elements of the protein. This mutation (R28A) is located at the subunit-subunit interface and it causes the disruption of salt bridges and hydrophobic contacts at the interface.

Materials and Methods

Molecular Dynamics simulations. Dimeric and monomeric structural models of reduced and oxidized DJ-1 WT protein together with M26I, L166P[*], R98Q and R28A were constructed based on the DJ-1 WT homodimer X-ray structure at a resolution of 1.95 Å (3).

In the oxidized form Cys and/or Met residues were assumed to be oxidized. We noticed that the shortest Cys-Cys distance (d[S-Cys53(A) and S-Cys53(B)]=3.2 Å) is too large for the formation of disulfide bridges. Thus, the three cysteines present in the protein (C46, C53 and C106) are replaced by cysteine sulphonic acid (31) (Fig. 1A). The four methionines (M17, M26, M133 and M134, Fig. 1A) are oxidized to methionine sulfoxide (18, 22) or methionine sulfone (22). We further noticed that neither the cysteine residues nor the methiones interact directly with residues involved in the PD mutations. Several models were considered, based

on the suggestion of Refs. (18, 22, 31): (i) the protein with all the Cys residues oxidized and all the Met reduced (WT-OX_1); (ii) the protein with all the Cys oxidized and all the Met oxidized to methionine sulfoxide (WT-OX_2); (iii) the protein with all the Cys oxidized, two methionines (M26 and M134) oxidized to methionine sulfoxide and the remaining two (M17 and M133) oxidized to methionine sulfone (WT-OX_3).

The point mutations were obtained by simple residue substitution, taking care that the substituted residue would not clash with the rest of the protein and that the χ_1 and χ_2 torsion angles would fall in the most energetically favorable regions (39, 40). The mutations in the dimeric structures were carried out for both subunits in order to obtain homodimers.

The proteins were immersed in a water box of edges ca. 69.0 Å x 66.0 Å x 69.0 Å and 81.0 Å x 76.0 Å x 94.0 Å for the monomeric and dimeric forms respectively. The solvent molecules were not included if the distance between any solvent atom and any protein atom was lower than the sum of their respective van der Waals' radii. Two or three sodium counterions were added to neutralize the systems. They were located in the regions of minimum electrostatic potential energy as calculated with the xleap program of the AMBER8 package (41, 42), namely close to Glu 59 and Asp 189. Periodic boundary conditions (PBC) were applied.

The AMBER99 (43, 44) and TIP3P (45) force fields were used for biomolecules with counterions and water respectively. The particle mesh Ewald method (PME) was applied to evaluate the long-range electrostatic interactions (46-48). A cutoff of 8 Å was used for both the real part of the electrostatic interaction and the van der Waals non-bonded interaction evaluation. A timestep of 2 fs was applied to propagate nuclear degrees of freedom. The SHAKE algorithm (49) was used to fix all bond lengths. The investigated models first underwent 10,000 steps of energy minimization. Then, the systems were equilibrated at constant temperature and pressure for at least 0.5 ns. Subsequently, our models underwent MD simulations with constant temperature and volume for at least 10.0 ns. Constant temperature conditions were obtained by using a Langevin

3

thermostat (50) at a target temperature of 300K with a coupling coefficient of 5 ps^{-1}. Constant pressure conditions were achieved with a Nosé-Hoover Langevin barostat (51, 52). For the barostat, an oscillation period of 200 fs was used and the damping timescale used was 100 fs.

All calculations were performed using the NAMD program (53). The obtained results have been further analyzed using the Gromacs (54, 55) and VMD (56) packages.

Computational Alanine Scanning. Mutations destabilizing subunit-subunit interactions in the DJ-1 dimeric form were identified using Baker's Alanine Scanning procedure (57, 58). This approach calculates the van der Waals and the electrostatic contributions to the free energy of binding. Binding energy hot spots are defined for residues at the subunit-subunit interface, whose Ala mutation causes a loss of free energy of the subunit-subunit interface greater or equal to 1 kcal/mol. The latter residues were defined as (57, 58): (i) residues that have at least one atom within a sphere with a 4 Å radius centered on an atom belonging to the other partner; (ii) residues that, upon dimer formation, become significantly buried, i.e. there is a significant increase in the number of C$_\beta$ atoms located within an 8 Å sphere centered on the C$_\beta$ atom of the analyzed residue (exposed 0–8, intermediate 9–14, and buried >14). The mutation causing the largest destabilization of the dimer (R28A) was selected for subsequent MD simulations according to the protocol described in the previous subsection.

Preparation of DJ-1 R28A mutant. A first PCR amplification has been performed using pcDNA3-DJ1WT (kindly provided by P. Rizzu) as the template and the primers DJ1R28A F1 (cggtcatccctgtagatgtcatgagggcagct) and FLAG DJ1 REV (gcgcgctctagactagtctttaagaacaagtgg). The purified PCR product served as the template for a second PCR amplification using the following primer:
DJMET26 F2:
Atatagaattcgcttccaaaagagctctggtcatcctggctaaaggag cagaggaaatggagacggtcatccctgtagat
in combination with FLAG DJ1 REV, in order to obtain the complete mutant sequence. After digestion with EcoRI and XbaI, a PCR fragment was ligated to a pcDNA3-2xFLAG vector, previously prepared in the laboratory.

Cross-linking assay. Human HEK 293 cells were transiently transfected using the calcium phosphate method with pCDNA3-2xFLAG-DJ-1 WT, L166P, M26I and R28A plasmids. 48 hours after transfection cells were extensively washed with PBS and harvested in lysis buffer (0.5% Triton X-100 in PBS) supplemented with 1X Complete protease inhibitor cocktail (Roche). Lysates were rotated at 4°C for 30 minutes, and soluble cell lysates were obtained by centrifugation at 13000 rpm for 30 minutes at 4°C. Protein content in each lysate was determined by the Bredford method (Biorad). Equal quantities of lysate (100 micrograms) were incubated with 5 mM disuccinimidyl suberate (DSS) (Pierce) or dimethyl sulfoxide (DMSO) control for 30 minutes at room temperature. The reaction was quenched by incubation with 50 mM Tris-HCl pH 7.5 for 15 minutes at room temperature. Lysates (5 micrograms) were analyzed by western blotting with an anti-FLAG antibody. Densitometric analysis was performed to quantify ratios between monomeric and dimeric DJ-1.

Co-immunoprecipitation. HEK 293 cells were transiently transfected with pCDNA3-2xFLAG- and pCDNA3-HA- vectors encoding DJ-1 WT, L166P, M26I and R28A and, after 48 hours, cells were washed in PBS and harvested in lysis buffer as previously described. Equivalent soluble lysates (0.9 mg) were immunoprecipitated with an anti-HA monoclonal antibody for 2 hours at 4°C, followed by incubation with Sepharose-protein A for 1 hour at 4°C. Bound proteins were eluted with Laemli buffer and revealed by western blotting with an anti-FLAG antibody.

RESULTS

MD of the DJ-1 WT protein. Molecular dynamics simulations over an 11 ns timescale are used here to investigate the structure of the reduced and oxidized forms of the DJ-1 protein in aqueous solution. The simulations are performed for both the dimeric and monomeric forms of the reduced state and for the dimeric form of the oxidized state. In the latter state, either the Cys or the Met residues are assumed to be oxidized (22). The

4

obtained results are used as a reference for comparison with the corresponding mutants.

In the reduced state, the Root Mean Square Deviation (RMSD) values fluctuate for the last 5 ns of the MD run around a value of 1.8 ± 0.1 Å and 1.8 ± 0.2 Å for the dimer and the monomer, respectively (Fig. 1B.i and Tab. 1). The standard deviation (SD) value suggests that the monomer undergoes larger structural fluctuations than the dimer, pointing to a key stabilizing role of the subunit-subunit association. In particular, the association stabilizes the flexible N- and C-terminal fragments. The distance values between C_{α} of the residues 1 and 189 fluctuate between 23 Å and 32 Å for the dimer while for the monomeric form they are between 20 Å and 34 Å (Fig. 1B.ii). The average distance is 27.5 Å (Fig. 1B.ii) for both forms. The secondary structure found in the X-ray experiments is conserved in both cases. Most of the subunit-subunit hydrogen bonds, along with the hydrophobic interactions and salt bridges are conserved during the entire MD run (Tab. 1SI). However, a salt bridge between Asp 24 and Arg 48, not detected in the X-ray structure, is formed after a few hundred ps of dynamics. The average distance between the centers of mass of the DJ-1 subunits in the model structure is 28.1 ± 0.3 Å while it is 27.9 Å in the X-ray structure of the DJ-1 protein (Fig. 1B.iii).

Several oxidized forms of the dimeric protein are considered, following previous work (18, 22, 31): (i) a form in which the cysteines are oxidized to cysteine sulphonic acid (WT-OX_1), (ii) one in which the cysteines are oxidized to cysteine sulphonic acid and the methionines oxidized to methionine sulfoxide (WT-OX_2) and (iii) one in which the cysteines are oxidized to cysteine sulphonic acid, two methionines (M26 and M134) oxidized to methionine sulfoxide and the remaining two (M17 and M133) oxidized to methionine sulfone (WT-OX_3) (22).

Our MD simulations show that such forms are fairly similar to the reduced form: (i) the RMSD ranges between 1.4 Å and 1.7 Å (Tab. 1), to be compared with 1.8 ± 0.1 Å of the WT in the reduced state; (ii) the contacts at the subunit-subunit interface are rather similar to those of the DJ-1 reduced form in aqueous solution (Tab. 1SI);

(iii) the MD-averaged distance between the centers of mass range between 28.0 Å and 29.1 Å (Fig. 1B), similar to the value of the reduced state (28.1 ± 0.3 Å); (iv) the solvent accessible surface area (SASA) (59, 60) for each subunit is similar to that of the reduced form (MD-averaged values ranging from 9,854 Å^2 to 10,150 Å^2, to be compared with 10,160 Å^2 for the reduced state).

We conclude that the oxidized and reduced forms of the DJ-1 protein in aqueous solution are very similar to the reduced form in the solid state.

MD of PD-causing DJ-1 mutations. Here we focus on the most studied PD-linked mutations: M26I and L166P (5-7, 13, 29, 35, 36). Because the estimation of the free energy difference between the WT and these mutants in the dimeric and oligomeric states by MD is not possible at the present stage, we adopt here a simple approach which can provide some indirect hints: first, we compare MD results on the mutant monomers to the monomeric WT in the reduced state[†] in aqueous solution. Within the limitation of the timescale investigated (~10 ns), we make the plausible assumption that the way the monomers assemble in the dimeric structure may be similar to the WT if the structural determinants of mutant monomers are similar to those of the WT in the monomeric state.

In that case, we use the WT dimeric X-ray structure (3) to construct the structure of the dimer mutants and investigate the stability of the dimer by MD simulations.

The RMSD of the M26I monomer turns out to be fairly similar to that of the WT in the monomeric state: it fluctuates around 1.9 Å over the last 5 ns, and the value at the end of the dynamics ranges between 1.6 Å - 2.5 Å (Tab. 1 and Fig. 3A). The secondary structure elements are fully maintained during the dynamics and the overall fold is similar to the WT (Fig. 2B).

Next, we compare structural determinants of the protein surface involved in the dimerization with those of the WT: (i) the distance (D) between the centers of mass of the secondary structure elements located at the interface (α1 helix and β3 β-sheet in Fig. 1A) is similar to that of the WT (D = 15.0 ± 0.6 Å vs 14.8 ± 0.5 Å respectively, see

5

Fig. 3B); (ii) the Root Mean Square Fluctuation (RMSF) per residue for M26I is very similar to that of the WT (Fig. 4). The similarity between the WT and M26I can be rationalized observing that the mutation does not affect the intramolecular interactions (Tab. 2SI). The interactions formed by M26 in the WT are the same as those formed by I26 in the mutant, since the methionine and isoleucine have similar volume and shape (61, 62) (Tab. 3SI).

We conclude that the interface of the M26I mutant has a similar conformation to the WT and subsequently, has a similar tendency to form dimers.

We then proceed to investigate the dimeric structure of M26I. The RMSD value of M26I in the dimeric state is similar to that of the WT (Tab. 1 and Fig. 2ASI) oscillating around 1.7 Å. The secondary structural elements are fully conserved during the molecular dynamics simulations. The non-bonded interactions at the subunit-subunit interface are also conserved during the MD run, analogously to the WT (Tab. 3SI). In addition, the centers of mass distance analysis showed that the distance between subunits in the mutant is similar to the distance between subunits obtained for the dimeric form of the WT (Fig. 2BSI). The local interactions around residue 26 are also fully conserved (Tab. 2SI). Finally, the SASA for each subunit is similar to the WT (average value: 10,203 $Å^2$ and 10,160 $Å^2$ respectively).

Thus, both the monomeric and dimeric forms of M26I are similar to the WT.

L166P monomer shows a different behaviour than the M26I monomer. Its RMSD exhibits larger fluctuations than in other mutants (Fig. 3A and Tab. 1). In addition, properties (i)-(ii) are different from that obtained for the WT: (i) the distance (D) between α1 helix and β3 β-sheet is smaller (D =12.5 ± 0.4 Å and 14.8 ± 0.5 Å, Fig. 3B); (ii) the RMSF of Asp 49 (located on the subunit surface involved in the dimerization process) is larger (Fig. 4). The discrepancies may be caused, as already suggested (4, 36), by the fact that the replacement of Leu with Pro disrupts α8 helix and therefore the local interactions of residue 166 are different (Tab. 2SI).

Thus, our results suggest the lowered dimerization efficiency of the L166P mutant may be due to structural differences in the monomer. These results are valid within the limits of the computational power of our analysis.

MD of R98Q physiological variant. Since it is a physiological variant of the DJ-1, R98Q is expected to alter none of DJ-1's biochemical functions (8). From a structural point of view, the replacement of R98, which is indeed exposed to the solvent, with a polar residue such as Q should not dramatically affect the thermodynamic stability of the protein. To investigate the effect of such a mutation, we follow the same computational protocol as for the PD-causing mutations.

The mutant monomer shows a similar behaviour to the WT form. Its RMSD does not show any large fluctuation compared to the WT (Fig. 3A and Tab. 1). In addition, properties (i)-(ii) are similar to those of the WT: (i) the distance (D) between α1 helix and β3 β-sheet is comparable to that of the WT (14.9 ± 0.5 Å and 14.8 ± 0.5 Å respectively, Fig. 3B); (ii) the RMSF shows a similar behaviour to those of the WT and M26I mutation (Fig. 4). Furthermore, the RMSD value of the dimeric form is comparable to that of the WT dimer (Tab. 1 and Fig. 2ASI) oscillating around 1.4 Å with small fluctuations after 5 ns. The behaviour of this physiological variant is similar to that of the dimeric forms of the DJ-1 WT and of the M26I mutant (Tab. 3SI). The analysis of centers of mass distance shows that the DJ-1 variant behaves similarly to the DJ-1 WT (Fig. 2BSI). Finally, the SASA for each subunit is similar to that of the WT (average value: 10,040 $Å^2$ and 10,160 $Å^2$, respectively).

Within the limitations of our approach, we conclude that R98Q variation, like the M26I, affects neither the dimeric nor the monomeric structures of the WT.

Computational identification of a dimer-incompetent DJ-1 mutation. Our calculations suggest that L166P is the only mutation among those considered that may alter dimer stability by modifying the fold of the single subunits. These in

6

turn might assemble differently than the WT to form HMW structures.

Here we attempt to identify a mutation that does affect stability by disrupting none of the secondary structure elements. We perform Baker's Computational Alanine Scanning procedure (57), which may quickly (albeit approximately) estimate changes in the interaction free energy ($\Delta\Delta G$) between the two subunits upon mutation of each interface residue with Ala. The largest $\Delta\Delta G$ value turns out to be associated with the R28A mutation (Tab. 2). This value is indeed twice as large than any other Ala substitutions presented in Table 2.

Following the MD protocol adopted for the other mutations, we have investigated by MD simulation the structural properties of the R28A monomeric form and we compared them to those of the WT monomer MD structure. The R28A monomer turns out to be similar to the WT: the RMSD value oscillates around 1.8 Å after 5 ns (Tab. 1 and Fig. 5A). In addition, properties (i)-(ii) are similar to those of the WT: (i) the distance (D) between the α1 helix and the β3 β-sheet is comparable to that of the WT (14.9 ± 0.5 Å and 14.8 ± 0.5 Å for the R28A mutant and the WT DJ-1, see Fig. 3B); (ii) the RMSF is similar to those of the WT and the M26I proteins (Fig. 4). The proteins fully maintain the secondary structure elements (Fig. 2B, Fig. 1SI). This is expected as the mutation is on the surface of the monomer.

We proceed then to investigate the dimeric form of R28A by MD simulation (Fig. 5B). The mutation deeply destabilizes the subunit-subunit interactions and the mutant shows a completely different behaviour compared to that of the WT protein: (i) The distance between the subunit centers of mass along with the SASA increases during the dynamics: at the end of the simulation it is much larger than those of the WT (Fig. 5). This suggests that the structure is evolving towards another minimum, in which the subunit-subunit interaction is less strong than in the WT. Unfortunately, observing an eventual complete detachment of the two subunits is well beyond the present domain of applications of MD simulations; (ii) consistently, the RMSD value increases during the dynamics up to 3.0 Å (Fig. 5B), which is significantly larger than the final value found for the WT (1.9 Å, Tab. 1 and Fig. 5B). Thus, it is not correct to take the average values of the RMSD (the structure is still evolving). We then calculate for this mutant the average value of the RMSD and the standard deviation (SD) of each subunit during the MD run. The values are 2.0 ± 0.5 Å for both subunits in the mutant, to be compared with 1.6 ± 0.1 Å and 1.7 ± 0.1 Å for each subunit of the WT dimer in the reduced form. This suggests that the R28A DJ-1 mutant is more flexible than the WT.

In vitro biochemical assays. To compare quantitatively the ability of PD-causing mutations to form dimers *in vitro*, we performed chemical cross-linking experiments. Human HEK 293 cells were transfected with FLAG-tagged DJ-1 WT, M26I, L166P, and R28A (Fig. 6). Initially we performed pilot experiments to estimate the amount of steady-state protein synthesized by the cells. While we confirmed that the amount of L166P was 20-40% of the DJ-1 WT, we noticed that the levels of R28A were higher than those of WT (Fig. 6 A and B). Then, soluble lysates were treated with covalent chemical cross-linker DSS or with DMSO as control. To obtain a measure of the dimerization efficiency, we performed densitometry analysis and calculated the ratio between dimer to monomer and we compared the various mutants to WT. The amount of total lysates was normalized to obtain a similar quantity of DJ-1 protein in all samples. As shown in Fig. 6 C and D, we confirmed that the L166P mutant has an impaired capacity to form a homodimer, while displaying a tendency to exist as HMW complexes. The efficacy in L166P dimer formation was calculated to be 20% of the WT DJ-1 or even less, and the normalization to monomer expression excludes that the effect is only due to the intrinsic poor stability of the L166P protein. The M26I mutant behaved as shown by Moore *et al.* (36), since dimer formation capability is equivalent to that of the WT DJ-1. Under these conditions, we observed that in the R28A (computationally selected mutant) the ability to form dimers is impaired and reduced to 50% of DJ-1 WT.

We then examined the *in vitro* self-association of WT, M26I, L166P and R28A by co-immunoprecipitation of differentially tagged protein in HEK 293 cells. FLAG-tagged WT DJ-1 co-immunoprecipitated with HA-tagged protein

7

and similarly the FLAG-tagged M26I mutant co-immunoprecipitated with its HA-tagged version. In contrast, L166P was unable to do so. The R28A FLAG-tagged mutant could only partially immunoprecipitate with its HA-tagged form (data not shown).

DISCUSSION

Several mutations of the DJ-1 gene have been associated with familiar cases of PD (2, 6, 13). Some of them clearly result in a loss of function since no DJ-1 protein is synthesized due to large deletions and/or splicing errors. The molecular basis of neurodegeneration induced by a group of DJ-1 missense mutations is less clear. A working hypothesis in the field is that DJ-1 carries out its function as a dimer and that missense mutations impair the quantity of the dimeric DJ-1 in the cell (2, 3, 34, 35, 63). In addition, since oxidized DJ-1 has been found in *post mortem* brains of PD patients (22), it is of interest to determine the structural determinants of such modifications.

Here we have used MD simulations to assess the effects on DJ-1 protein structure of oxidative stress and of two missense mutations causing familiar PD (L166P, M26I) (9) along with a physiological variant (R98Q) (8).

Our MD simulations suggest that:

(i) WT in solution is very similar to the X-ray structure in both reduced and oxidized states and in both monomeric and dimeric forms.

(ii) The M26I monomer is structurally similar to the WT monomer, because the mutation does not disrupt intra-protein interactions of the WT (Tab. 2SI). Thus, this monomeric structure may assemble similarly to the WT to form dimers.

(iii) The local conformation around P166 in the L166P monomer evolved towards a conformation significantly different from that of the WT. This might be due to the disruption of α8 helix, which in turn affects the conformations of the secondary structure elements at the subunit-subunit interface (α1, α9 helices and β3 β-sheet). Thus, although P166 is not located at the subunit surface involved in the dimerization, it changes its shape by modifying some of the intra-protein interactions. This is shown by a comparison of structural determinants of the protein surface of the mutant with the WT (Tab. 2SI). The different conformation of L166P monomeric units might

affect the mutant's ability to assemble in dimeric and multimeric structures. Indeed, by gel filtration and other assays, L166P has been previously shown to be present mostly as an HMW complex that may contain either DJ-1 oligomers and/or aggregates with other proteins (5, 33, 35). This led to the hypothesis that L166P may have additional, unidentified, dominant-negative effects. Parkin, CHIP and hsp70 were all able to interact with L166P as part of a large complex (34). Furthermore, Parkin interaction provoked the sequestration of DJ-1 mutants into insoluble fractions (34). By *in vitro* experiments we confirmed previous data that the ectopic expression of L166P is very low and that dimer formation is very negligible. Interestingly, we detected the previously identified HMW complex that may be involved in abnormal oligomerization and protein/protein interactions (5, 33, 35).

(iv) MD simulations show that the dimeric structures of M26I and R98Q DJ-1s are similar to that of the WT and they keep the subunit-subunit interactions intact. The dimeric structures turn out to be less flexible than the monomer, especially in the flexible N- and C-terminal fragments. This fact points to a stabilizing role of the subunit-subunit association.

These results for M26I are consistent with our *in vitro* assays, which show that M26I has the same ability as WT to form dimers. Therefore, our combined computational and experimental approach, along with previous experimental work (5, 7), provides a coherent picture in which M26I assumes mostly a dimeric structure. The results for R98Q are consistent with the fact that this mutant is a physiological variant.

We conclude that the PD-causing M26I mutation does not largely affect the stability of the dimer and does not destabilize it by changing the shape of the subunit-subunit contact surface.

To identify a mutation that decreases the affinity for the dimeric structure without changing the fold of the monomer, we next perform Baker's Computational Alanine Scanning procedure (57) and MD calculations. We find that R28A is indeed able to cause destabilization at the interface. Furthermore, the MD structure of the R28A monomer turns out to be similar to that of the WT monomer, as shown by the comparison of selected

structural determinants (Fig. 3B and Fig. 4AB). This may be caused by the fact that A28 faces the solvent. However, the MD simulations point to the destabilization of the dimer as already observed in the timescale investigated (~10 ns).

The SASA for water and the distances between the centers of mass increase on passing from the WT to R28A (Fig. 5D). This is caused by the disruption of subunit-subunit interactions, rather than a change of shape of the subunit surface. The computational results are consistent with *in vitro* experiments that showed R28A has a reduced, although not abolished, capacity to form homodimers as compared to DJ-1 WT. This effect is not caused by a reduced stability of the R28A mutant since the protein is expressed at even higher levels than the DJ-1 WT (Fig. 6 A and B).

CONCLUDING REMARKS

We have presented combined computational and experimental investigations of two PD-causing DJ-1 mutations: M26I and L166P.

M26I affects neither the monomeric structure nor the dimeric one (7). Furthermore, our results show that the mutant has a similar tendency to form dimers as that of the WT.

The L166P mutation favors the formation of multimers against the dimeric structure (5, 34, 35).

This is probably due to the different conformation of the monomeric subunit (3). The mutated residue is indeed located not at the subunit-subunit interface, but rather on α8 helix. Thus, oligo- or monomer L166P may form *in vivo* and present a different pattern of protein-protein interactions than DJ-1 WT (see Figs. 3 and 4). Although this issue cannot be firmly established with calculations alone, it is supported experimentally here and in the work of others (34). The relevance of these interactions will probably depend on the L166P protein level *in vivo*. It must be noted that to the best of our knowledge no investigation of DJ-1 L166P protein has been done in *post mortem* brains of PD patients carrying this mutation or in *knock-in* animal models. It will be interesting to investigate whether L166P *in vivo* is unstable or a component of HMW aggregates.

Our investigation is complemented by a search for mutations that decrease the affinity for the dimer without affecting the fold of the DJ-1 protein.

In conclusion, this work presents MD simulations for L166P, M26I and R28A DJ-1 protein mutants, giving an insight into their molecular structures and properties. This computational study is supported by biochemical *in vitro* data.

REFERENCES

1. Moore D.J., West A.B., and Dawson T.M. (2005) *Annu. Rev. Neurosci.* **28,** 57-87
2. Lev N., Roncevich D., Ickowicz D., Melamed E., and Offen D. (2006) *J. Mol. Neurosci.* **29,** 215-225
3. Honbou K., Suzuki N.N., Horiuhci M., Niki T., Taira T., Ariga H., and Inagaki F. (2003) *J. Biol. Chem.* **278,** 31380-31384
4. Wilson M.A., Collins J.L., Hod Y., Ringe D., and Petsko G.A. (2003) *Proc. Natl. Acad. Sci. U S A.* **100,** 9256-9261
5. Baulac S., LaVole M.J., Strahle J., Schiossmacher M.G., and Xia W. (2004) *Mol. Cell. Neurosci.* **27,** 236-246
6. Abou-Sleiman P.M., Healy D.G., Quinn N., Lees A.J., and Wood N.W. (2003) *Ann. Neurol.* **54,** 283-286
7. Blackinton J., Ahmad R., Miller D.W., van der Brug M.P., Canet-Aviles R.M., Hague S.M., Kaleem M., and Cookson M.R. (2005) *Mol. Brain Res.* **134,** 76-83
8. Hedrich K., Schafer N., Hering R., Hagenah J., Lanthaler A.J., Schwinger E., Kramer P.L., Ozellus L.J., Bressman S.B., Abbruzzese G., Martinelli P., Kostic V., Pramstaller P.P., Vieregge P., Taanman J.W., Riess O., and Klein C. (2004) *Ann. Neurol.* **55,** 145-146
9. Cookson M.R. (2005) *Ann. Rev. Biochem.* **74,** 29-52
10. Lang A.E. and Lozano A.M. (1998) *New Engl. J. Med.* **339,** 1044-1053
11. Lang A.E. and Lozano A.M. (1998) *New Engl. J. Med.* **339,** 1130-1143

12. Pankratz N. and Foroud T. (2004) *NeuroRx.* **1,** 235-242
13. Bonifati V., Rizzu P., van Baren M.J., Schaap O., Breedveld G.J., Krieger E., Dekker C.J., Squitieri F., Ibanez P., Joose M., van Dongen J.W., Vanacore N., van Switen J.C., Brice A., Meco G., van Duijin C.M., Oostra B.A., and Heutink P. (2003) *Science* **299,** 256-259
14. Le Naour F., Misek D.E., Krause M.C., Deneux L., Giordano T.J., Scholl S., and Hanson M. (2001) *Clinical Cancer Research* **7,** 3328-3335
15. Allard L., Burkhard P.R., Lescuyer P., Burgess J.A., Walter N., Hochstrasser D.F., and Sanchez J.C. (2005) *Proteomics and Protein Markers* **51,** 2043-2051
16. Inden M., Taira T., Kitamura Y., Yanagida T., Tsuchiya D., Takata K., Yanagisawa D., Nishimura K., Tanaguchi T., Kiso Y., Yoshimoto K., Agatsuma T., Koide-Yoshida S., Iguchi-Ariga S.M., and Shimohama S.Ariga H. (2006) *Neurobiol. Dis.* **24,** 144-158
17. Waragai M., Wei J., Fujita M., Nakai M., Ho G.J., Masliah E., Akatsu H., Yamada T., and Hashimoto M. (2006) *Biochem. Biophys. Res. Commun.* **345,** 967-972
18. Zhou W., Zhu M., Wilson M.A., Petsko G.A., and Fink A.L. (2006) *J. Mol. Biol.* **356,** 1036-1048
19. Xu J., Zhong N., Wang H., Elias J.E., Kim C.Y., Woldman I., Pifl C., Gygi S.P., Geula C., and Yankner B.A. (2005) *Hum. Mol. Genet.* **14,** 1231-1241
20. Taira T., Saito Y., Niki E., Iguchi-Ariga S.M., Takahashi K., and Ariga H. (2007) *EMBO Rep* **5,** 213-218
21. Bandopadhyay R., Kingsbury A.E., Cookson M.R., Reid A.R., Evans I.M., Hope A.D., Pittman A.M., Lashley T., Canet-Aviles R., Miller D.W., McLendon C., Strand C., Leonard A.J., Abou-Sleiman P.M., Healy D.G., Ariga H., Wood Nicholas W., de Silva R., Revesz T., Hardy J.A., and Lees A.J. (2007) *Brain* **127,** 420-430
22. Choi J., Sullards M.C., Olzmann J.A., Rees H.D., Weintraub S.T., Bosrwick D.E., Gearing M., Levey A.I., Chin L.S., and Li L. (2006) *J. Biol. Chem.* **281,** 10816-10824
23. Hague S.M., Rogaeva E., Hernandez D., Gulick C., Singleton A., Hanson M., Johnson J., Weiser R., Gallardo M., Ravina B., Gwinn-Hardy K., Crawley A., St George-Hyslop P.H., Lang A.E., Heutink P., Bonifati V., Hardy J.A., and Singleton A. (2003) *Ann. Neurol.* **54,** 271-274
24. Meulener M.C., Xu K., Thomson L., Ischiropoulos H., and Bonini N.M. (2006) *Proc. Natl. Acad. Sci. U S A.* **103,** 12517-12522
25. Goldberg M.S., Pisani A., Haburcak M., Vortherms T.A., Kitada T., Costa C., Tong Y., Martella G., Tscherter A., Martins A., Bernardi G., Roth B.L., Pothos E.N., Calabresi P., and Shen J. (2005) *Neuron* **45,** 489-496
26. Kim R.H., Smith P.D., Aleyasin H., Hayley S., Mount M.P., Pownall S., Wakeham A., You-Ten A.J., Kalia S.K., Horne P., Westaway D., Lozano A.M., Anisman H., Park D.S., and Mak T.W. (2005) *Proc. Natl. Acad. Sci. U S A.* **102,** 5215-5220
27. Chen L., Cagniard B., Mathews T., Jones S., Koh H.C., Ding Y., Carvey P.M., Ling Z., Kang U.J., and Zhuang X. (2005) *J. Biol. Chem.* **280,** 21418-21426
28. Martinat C., Shendelman S., Jonason A., Leete T., Beal M.F., Yang L., Floss T., and Abeliovich A. (2004) *PLoS Biol.* **2,** 1754-1763
29. Gorner K., Holtorf E., Waak J., Pham T.T., Vogt-Weisenhorn D.M., Wurst W., Haass C., and Kahle P.J. (2007) *J. Biol. Chem.* **Epub,**
30. Takahashi K., Niki T., Taira T., Iguchi-Ariga S.M., and Ariga H. (2004) *Biochem Biophys Res Commun* **320,** 389-397
31. Kinumi T., Kimata J., Taira T., Ariga H., and Niki E. (2004) *Biochem. Biophys. Res. Commun.* **317,** 722-728
32. Canet-Aviles R.M., Wilson M.A., Miller D.W., Ahmad R., McLendon C., Bandyopadhyay S., Baptista M., Ringe D., Petsko G.A., and Cookson M.R. (2004) *Proc. Natl. Acad. Sci. U S A.* **101,** 9103-9108
33. Macedo M.G., Anar B., Bronner I.F., Cannella M., Squitieri F., Bonifati V., Hoogeveen A., Heutink P., and Rizzu P. (2003) *Hum. Mol. Genet.* **12,** 2807-2816

10

34. Moore D.J., Zhang L., Troncoso J., Lee M.K., Hattori N., Mizuno Y., Dawson T.M., and Dawson V.L. (2005) *Hum. Mol. Genet.* **14,** 71-84
35. Olzmann J.A., Brown K., Wilkinson K.D., Rees H.D., Huai Q., Ke H., Levey A.I., Li L., and Chin L.S. (2004) *J. Biol. Chem.* **279,** 8506-8515
36. Moore D.J., Zhang L., Dawson T.M., and Dawson V.L. (2003) *J. Neurochem.* **87,** 1558-1567
37. Bonifati V., Oostra B.A., and Heutink P. (2004) *J. Mol. Med.* **82,** 163-174
38. Miller D.W., Ahmad R., Hague S., Baptista M., Canet-Aviles R., McLendon C., Carter D.M., Stadler J., Chandran J., Klinefelter G.R., Blackstone C., and Cookson M.R. (2003) *J. Biol. Chem.* **278,** 36588-36595
39. Laskowski R.A., MacArthur M.W., Moss D.S., and Thornton J.M. (1993) *J. Appl. Cryst.* **26,** 283-291
40. Morris A.L., MacArthur M.W., Hutchinson E.G., and Thornton J.M. (2007) *Proteins* **12,** 345-364
41. Case D.A., Pearlman D.A., Caldwell J.W., Cheatham III T.E., Wang J., Ross W.S., Simmerling L., Darden T.A., Merz K.M., Cheng A.L., Vincent J.J., Crow-ley M., Tsui V., Gohlke H., Radmer R.J., Duan Y., Pitera J., Massova I., Seibel G.L., Singh U.C., Weiner P.K., and Kollman P.A. (2002) AMBER 8. University of California, San Francisco
42. Case D.A., Cheatham III T.E., Darden T., Gohlke H., Luo R., Merz K.M., Onufriev A., Simmerling C., Wang B., and Woods R.J. (2005) *J. Comput. Chem.* **26,** 1668-1688
43. Wang J., Cieplak P., and Kollman P.A. (2000) *J. Comput. Chem.* **21,** 1049-1074
44. Ponder J.W. and Case D.A. (2003) *Ann. Rev. Biochem.* **66,** 27-85
45. Jorgensen W.L., Chandrasekhar J., Madura J.D., Impey R.W., and Klein M.L. (1983) *J. Chem. Phys.* **79,** 926-935
46. Darden T., York D., and Pedersen L.G. (1993) *J. Chem. Phys.* **98,** 10089-10092
47. Essman U., Perela L., Berkowitz M.L., Darden T., Lee H., and Pedersen L.G. (1995) *J. Chem. Phys.* **103,** 8577-8592
48. Sagui C. and Darden T. (1999) *Annu. Rev. Biophys. Biomol. Struct.* **28,** 155-179
49. Ryckaert J.P., Ciccotti G., and Berendsen H.J.C. (1977) *J. Comp. Phys.* **23,** 327-341
50. Adelman S.A and Doll J.D. (1976) *J. Chem. Phys.* **64,** 2375-2388
51. Martyna, G. J., Tobias, D. J., and Klein, M. L. (1994) *Journal of Chemical Physics* **101,** 4177-4189
52. Feller S.E., Zhang Y., Pastor R.W., and Brooks B.R. (1995) *J. Chem. Phys.* **103,** 4613-4621
53. Phillips J.C., Braun R., Wang W., Gumbart J., Tajkhorshid E., Villa E., Chipot C., Skeel R.D., Kale L., and Schulten K. (2005) *J. Comput. Chem.* **26,** 1781-1802
54. Berendsen H.J.C., van-derSpoel D., and van-Drunen R. (1995) *Comp. Phys. Comm.* **91,** 43-56
55. Lindhal E., Hess B., and van der Spoel D. (2001) *J. Mol. Model.* **7,** 306-317
56. Humphrey W., Dalke A., and Schulten K. (1996) *J. Molec. Graphics* **14,** 33-38
57. Kortemme T., Kim D.E., and Baker D. (2004) *Sci. STKE* **219,** 1-8
58. Kortemme T. and Baker D. (2002) *Proc. Natl. Acad. Sci. U S A.* **99,** 14116-14121
59. Connolly M.L. (1983) *J. Appl. Crystallogr.* **16,** 548-558
60. Richmond T.J. (1984) *J. Mol. Biol.* **178,** 63-89
61. Janin J. (1979) *Nature* **277,** 491-492
62. Wolfenden R., Andersson P., Cullis P., and Southgate C. (1982) *Biochemistry* **157,** 105-132
63. Ariga H., Honbou K., Suzuki N.N., Horiuchi M., Niki T., Taira T., Ariga H., and Inagaki F. (2003) *J. Biol. Chem.* **278,** 31380-31384

FOOTNOTES

The abbreviations used in the text are: PD, Parkinson's disease; MD, molecular dynamics; WT, wild type; KO, knock-out; HMW, high molecular weight; PME, particle mesh Ewald method; PCR, polymerase chain reaction; PBS, Phosphate Buffered Saline; DSS, disuccinimidyl suberate; DMSO, dimethyl sulfoxide; RMSD, root mean square deviation; SD, standard deviation; RMSF, root mean square fluctuation; SASA solvent accessible surface area SASA

[*]For this mutant, only the monomer was built (see the Results section for details).
[†] We expect the mutant oxidized forms to be very similar to the reduced ones as shown by the MD simulations of the WT.

FIGURE LEGENDS

Figure 1. DJ-1 WT structure. (A) X-ray structure in the reduced state (3). The protein is a homodimer; each subunit assumes an α/β sandwich fold, similar to the Rossmann fold, conserved across the ThiJ-PfpI superfamily (3). The cysteine and methionine Cα atoms are shown as spheres. Labeling of selected secondary structure elements at the subunit-subunit interface (α1, α8, α9 helices and β3 β-sheet) as in Ref. (3). **(B)** Molecular dynamics of the protein in aqueous solution. i. Root mean square deviation (RMSD) from the corresponding initial structure of backbone atoms of the dimeric (black) and monomeric (red) forms plotted as a function of simulation time. ii. Distance between the N-terminal and the C-terminal C-α of the dimer (black) and of the monomer (red). iii. Distances between the centers of mass (COM) of subunits in the reduced (black) and oxidized states (green (WT-OX_1), yellow (WT-OX_2) and magenta (WT-OX_3), see Materials and Methods for details).

Figure 2. DJ-1 mutants investigated in this work. (A) Location of PD-causing mutations (M26I, L166P (1)) together with R98, which is mutated to Q in a physiological variant (8). **(B)** Structures obtained after 11 ns of MD simulations of M26I and L166P monomers (red line) superimposed on the corresponding structure of the WT monomer (blue line).

Figure 3. Selected properties of mutants in the monomeric state plotted as a function of time. (A) RMSD with respect to the initial structure. **(B)** Distance between the secondary structure elements at the subunit-subunit interface (defined in the text). Details of the computational protocol are given in the Materials and Methods section.
Color coding is as follows: WT: black, M26I: green, L166P: red, R98Q: blue, and R28A violet.

Figure 4. Fluctuations of mutant monomers. (A) RMSF of WT, M26I, R98Q, and L166P. **(B)** Close up of the region (residues 40 to 55) exhibiting the most significant residues fluctuations. Color coding as in Fig. 3.

Figure 5. Comparison between selected properties of WT and R28A, plotted as a function of time. RMSD of backbone atoms of the WT (black) and R28A mutant (red) for: **(A)** monomers and **(B)** dimers. **(C)** Distance between the centers of mass of subunits of the WT and R28A dimers. **(D)** Solvent accessible surface area for monomers (lower values) and dimers (larger values) of WT and R28A.

Figure 6. *In vitro* analysis of DJ-1 dimer formation. (A) HEK 293 cells were transiently transfected with FLAG-tagged DJ-1 contructs. Equal amount of total protein (5micrograms) was loaded on gel and

immunoblotted with anti-FLAG antibody. **(B)** Densitometric analysis of protein bands was performed using Adobe Photoshop 7.0 on two independent experiments. Relative expression was normalized to DJ-1wt protein. **(C)** HEK 293 cells were transfected as in A. Protein lysates were treated with chemical cross-linker DSS or with DMSO as indicated. Normalized quantities of transfected proteins were loaded on gel. Monomer, dimer and HMW forms of DJ-1 were visualized with anti-FLAG antibody. **(D)** Densitometric analysis of monomer and dimer bands was obtained by Adobe Photoshop 7.0 on two independent experiments. Dimer to monomer ratio was calculated and normalized to DJ-1wt protein.

TABLES

Table 1. Selected MD-averaged RMSD values of the DJ-1 WT and its mutants investigated in this study. For R28A, the RMSD increases during the dynamics and therefore only the final value is given.

RMSD [Å]	Dimer			Monomer		
	Average	SD	Final value	Average	SD	Final value
WT Reduced	1.8	0.1	1.9	1.8	0.2	2.1
WT-OX_1	1.6	0.1	1.7	---	---	---
WT-OX_2	1.4	0.1	1.5	---	---	---
WT-OX_3	1.6	0.1	1.6	---	---	----
L166P	---	---	---	2.0	0.2	1.9
M26I	1.7	0.1	1.7	1.5	0.1	1.8
R98Q	1.4	0.1	1.5	1.9	0.2	1.7
R28A	--	---	2.5	1.8	0.1	1.9

Table 2. Computational Alanine Scanning - based (57, 58) free energies obtained for the DJ-1 dimeric structure taken from X-ray experiments (3).

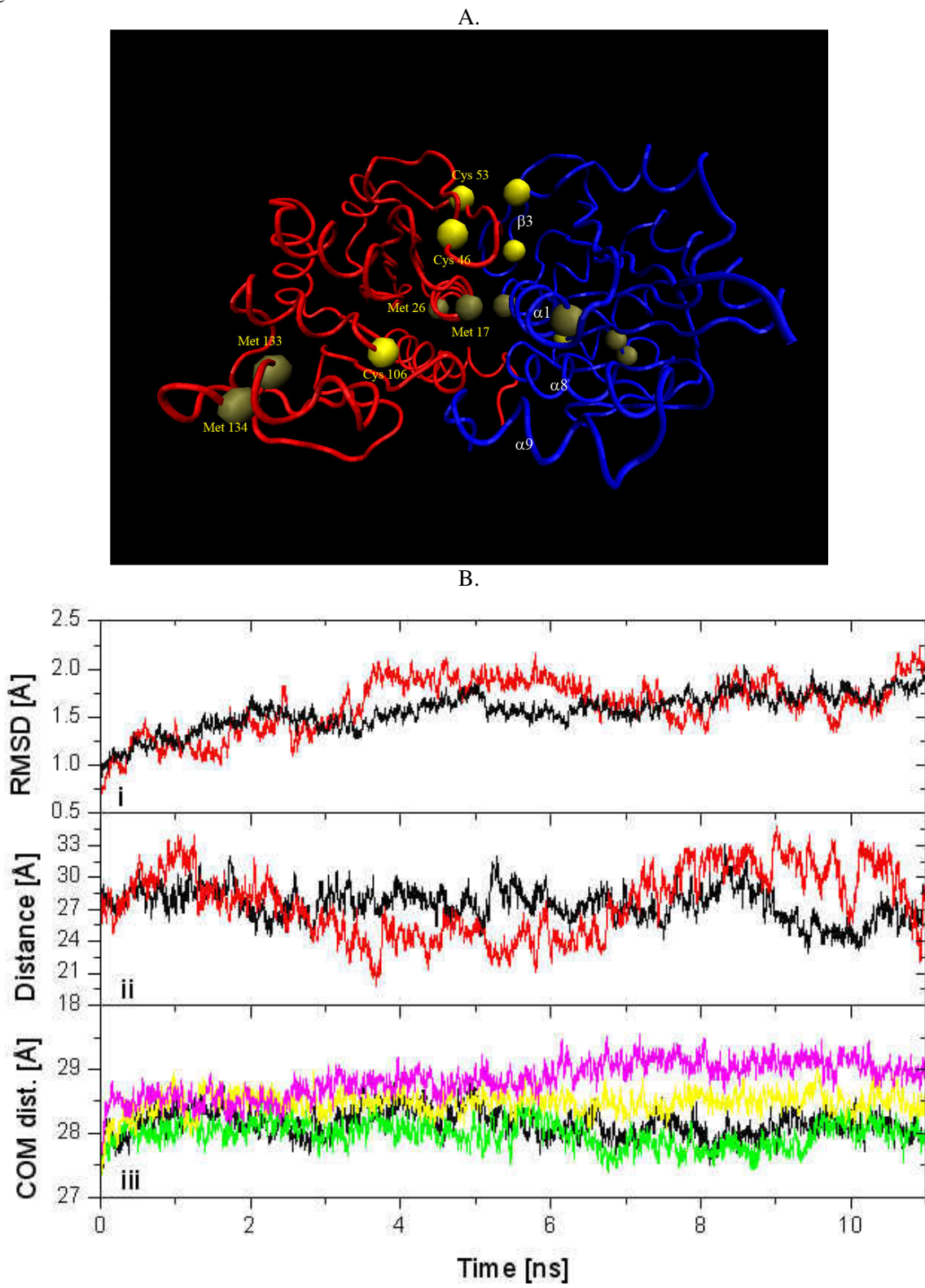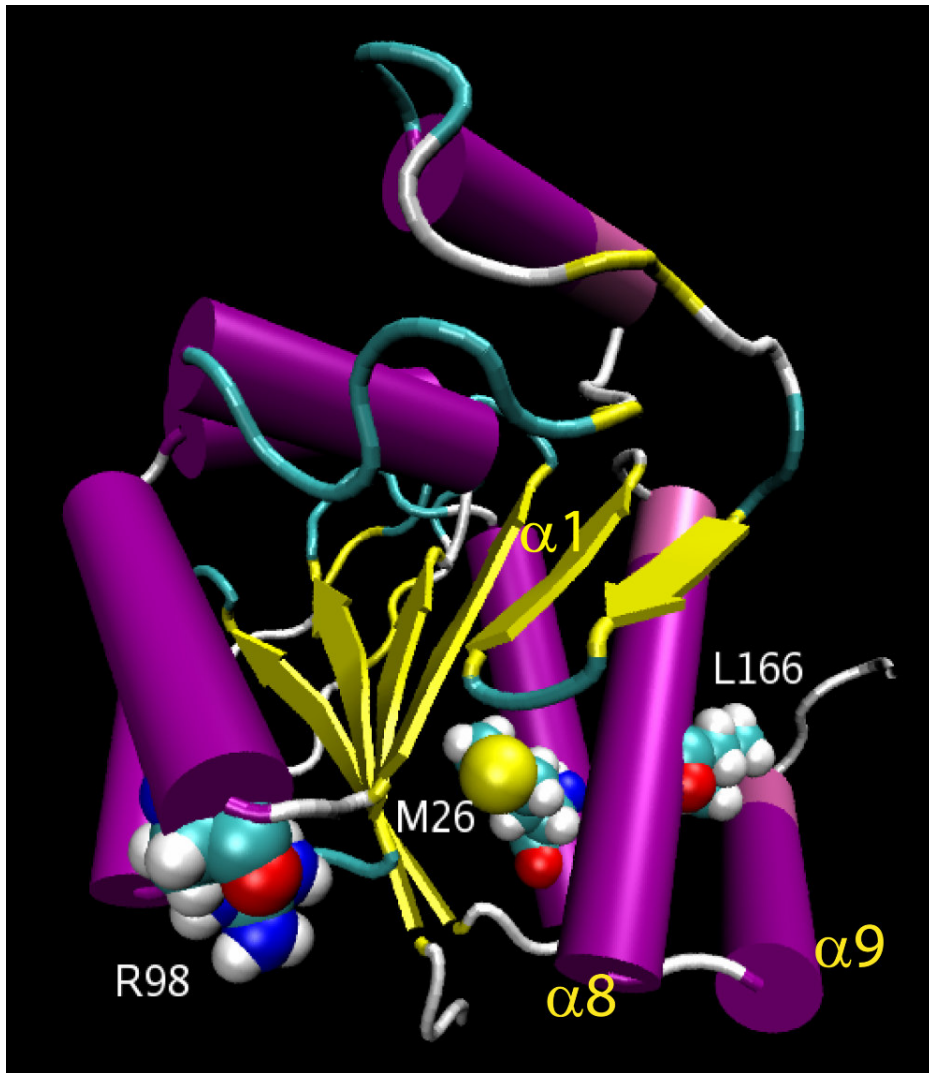| Residue	ΔΔG (bind) kcal/mol
M17	1.3
V20	1.3
R27	1.6
R28	**2.9**
V50	1.4
I52	1.1
G159	1.5
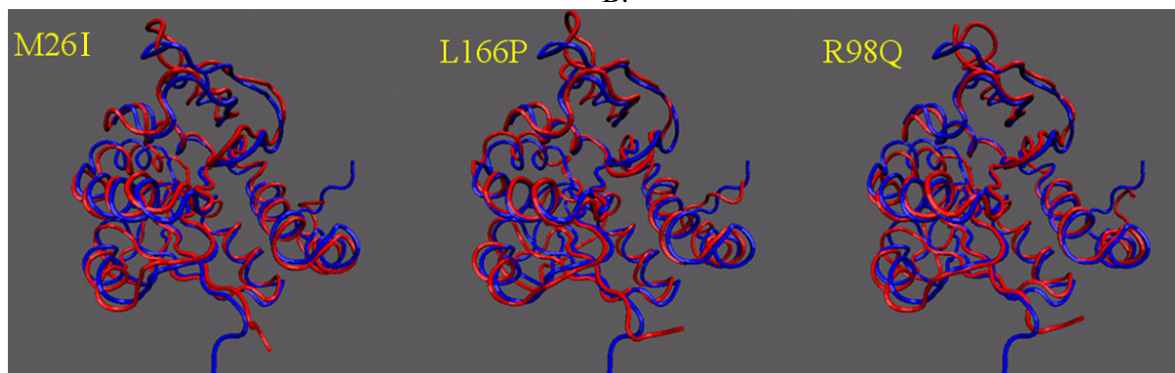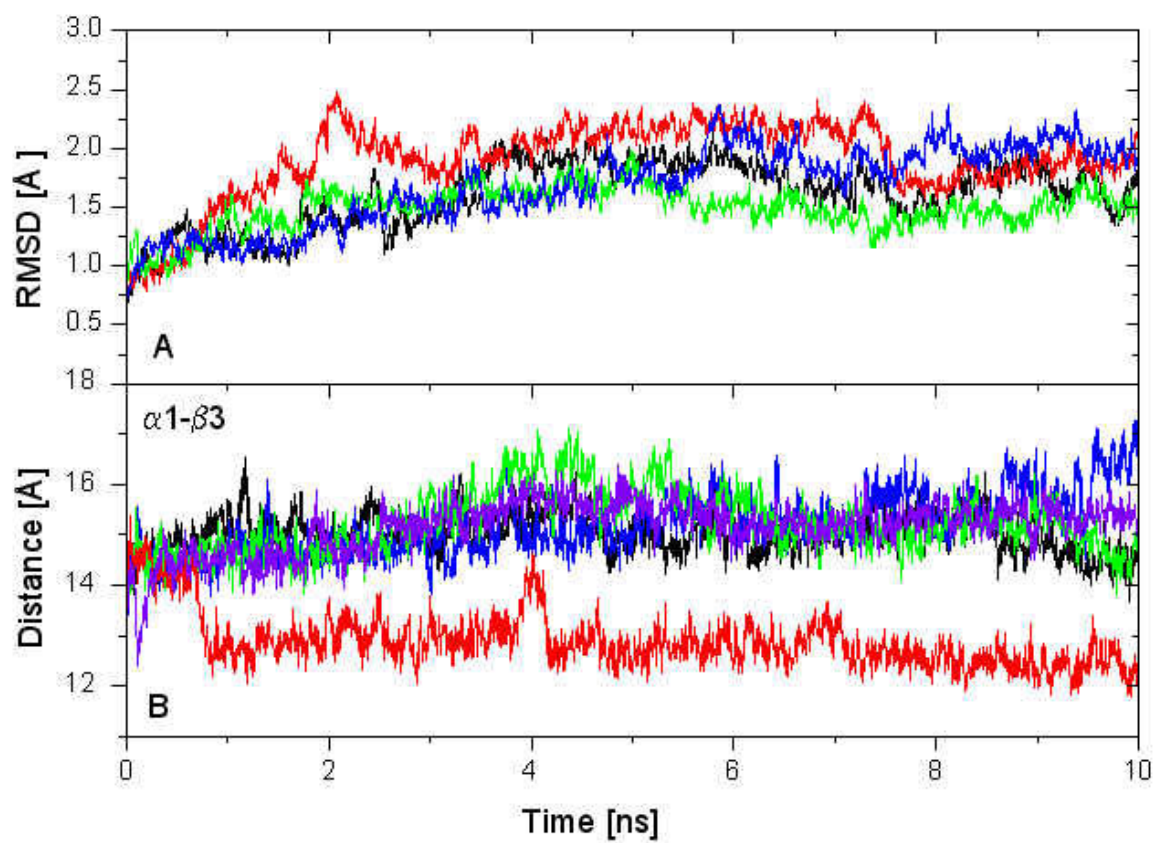
13

Figure 1

A.

B.

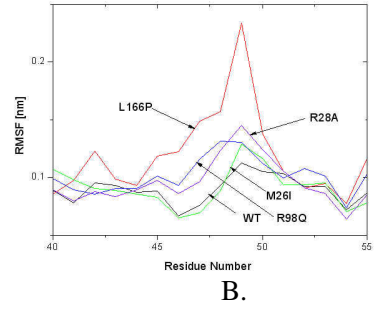Figure 2

A.

B.

15

Figure 3
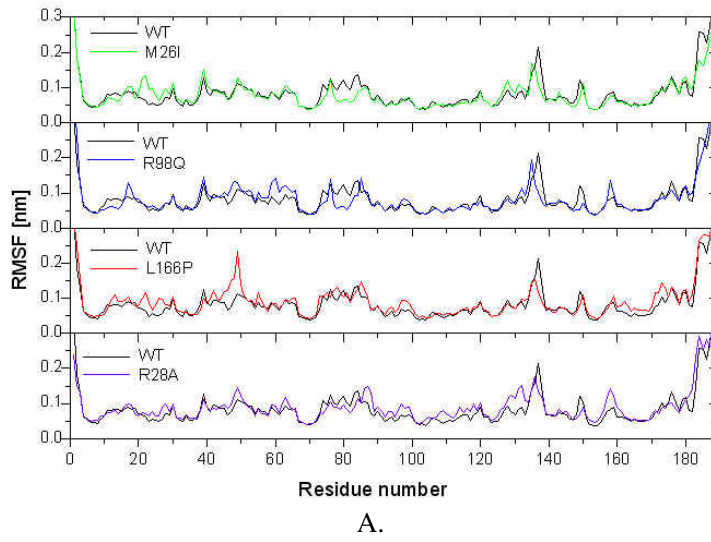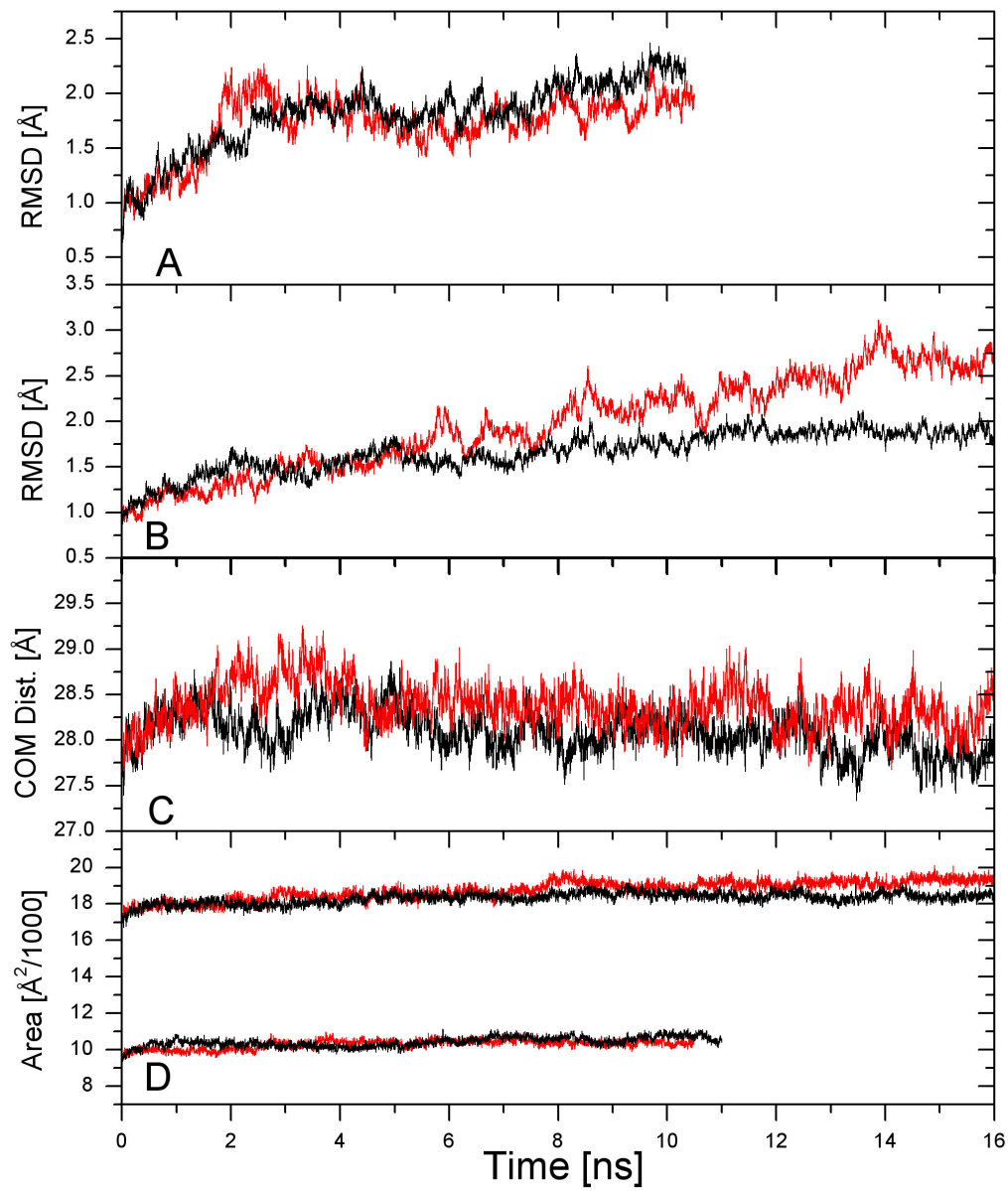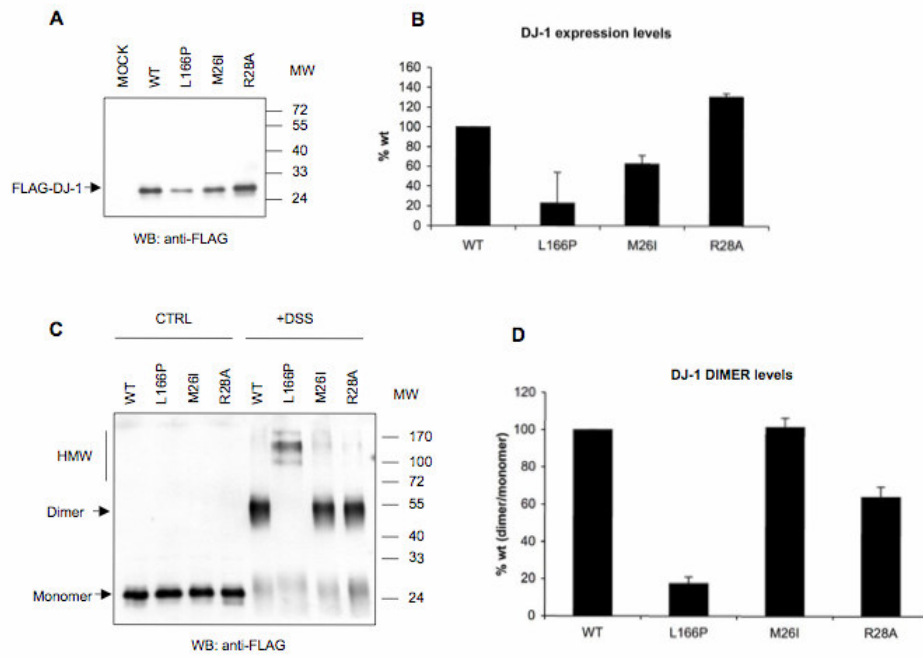
Figure 4

A.

B.

17

Figure 5

Figure 6

19

On the oligomeric state of DJ-1 protein and its mutants associated with Parkinson's Disease: a combined computational and in vitro study

Fernando E. Herrera, Silvia Zucchelli, Aneta Jezierska, Zeno Scotto Lavina, Stefano Gustincich and Paolo Carloni

J. Biol. Chem. published online May 15, 2007

Access the most updated version of this article at doi: 10.1074/jbc.M701013200

Alerts:
- When this article is cited
- When a correction for this article is posted

Click here to choose from all of JBC's e-mail alerts

Supplemental material:

http://www.jbc.org/content/suppl/2007/07/16/M701013200.DC1